DOI:10.22337/2587-9618-2025-21-4-130-145

NUMERICAL MODELING OF CAST-IN-PLACE REINFORCED CONCRETE BUBBLE DECK FLOOR SLABS UTILIZED IN EARTHQUAKE-PRONE REGIONS. PART TWO

Alexander M. Belostotsky [1,2]***, Alexander I. Nagibovich*** [1,2]***, Sergey V. Scherbina*** [1,2]***, Tatiana N. Vasileva*** [1,2]

[1] National Research Moscow State University of Civil Engineering, Moscow, RUSSIA
[2] Research & Development Centre StaDyO, Moscow, RUSSIA

Abstract: This article presents developed techniques for numerical modelling of lightweight cast-in-place reinforced concrete bubble deck floor slabs and a comparative analysis of different approaches to numerical modelling of buildings and structures with such lightweight floors, that are constructed in earthquake-prone regions.

Keywords: finite element method, modal analysis, earthquake excitation, mechanical safety, void formers, lightweight cast-in-place reinforced concrete floor slabs

ЧИСЛЕННОЕ МОДЕЛИРОВАНИЕ МОНОЛИТНЫХ ЖЕЛЕЗОБЕТОННЫХ ПЕРЕКРЫТИЙ С ПУСТОТООБРАЗОВАТЕЛЯМИ, ПРИМЕНЯЕМЫХ В СЕЙСМИЧЕСКИ АКТИВНЫХ РАЙОНАХ. ЧАСТЬ 2

А.М. Белостоцкий [1,2]***, А.И. Нагибович*** [1,2]***, С.В. Щербина*** [1,2]***, Т.Н. Васильева*** [1,2]

[1] Национальный исследовательский Московский государственный строительный университет, г. Москва, РОССИЯ
[2] АО «Научно-исследовательский центр СтаДиО», г. Москва, РОССИЯ

Аннотация: В настоящей статье представлены разработанные авторами методики численного моделирования облегченных монолитных железобетонных перекрытий с пустотообразователями и сравнительный анализ различных подходов к численному моделированию зданий и сооружений, строящихся в сейсмически активных районах и имеющих в своём составе подобные облегчённые плиты перекрытий.

Ключевые слова: метод конечных элементов, модальный анализ, сейсмическое воздействие, механическая безопасность, пустотообразователи, облегченные монолитные железобетонные перекрытия.

1. INTRODUCTION

A reinforced concrete bubble deck floor slab solution is widely used as a building design solution in earthquake-prone regions. Utilization of void formers is one of the ways to decrease the dead weight of concrete structures, that leads to reduced seismic loads and loads on vertical load-bearing structures and foundation.

The finite element method is widely used to solve structural mechanics problems, eigenvalue problems, and to perform a response spectrum analysis. The best way to extract eigenmodes and eigenfrequencies of a system with structural elements having complex cross-sections, to determine its stress-strain state is spatial discretization of such a system with solid elements. However, such a technique is computationally ineffective. Therefore, a common practice is to use structural finite elements, shell and beam ones, to spatially discretize a structural mechanics problem.

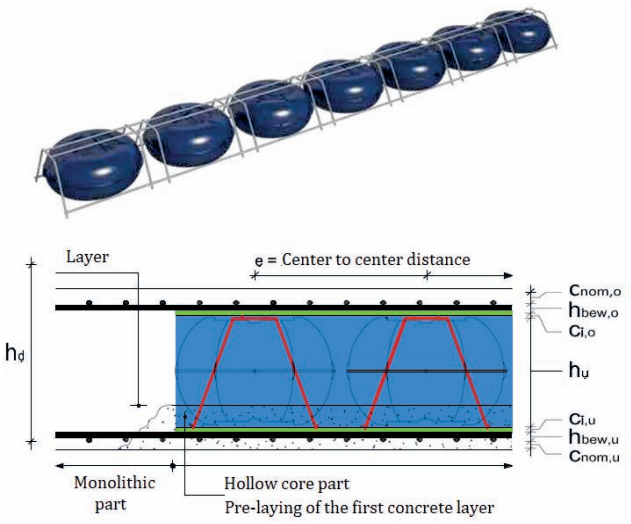


Figure 1. An example of void formers used in reinforced concrete floor slabs, and their geometrical parameters

The first part of the present research [1] has considered a single floor cell of a reinforced concrete frame building (see Fig. 2). The chosen part of the floor slab has dimensions of 5.6×5.6 meters and comprises 16 void former cells in each direction. The floor slab has the following values of its geometrical parameters: the floor slab thickness h_d = 250mm; the void former height h_u = 140mm; the concrete cover at the upper slab face $c_{nom,o}$ = 20mm; the concrete cover at the lower slab face $c_{nom,u}$ = 20mm; the distance between bubbles centers e = 350mm; the void former diameter d = 315mm. A cross-section of the single void former cell is shown in Fig. 3.

Properties of the considered bubble deck floor slab material are given in Table 1.

The verified ANSYS software [2] has been used for all simulations (a static loading analysis and a modal analysis). A reference finite element model of the simulated part of the floor slab has been assembled using solid finite elements of the type SOLID185 for spatial discretization of the problem. Corresponding mesh within the void former cell is illustrated in Fig. 4. Because only elastic part of the problem has been considered, utilization of the numerical solution obtained using the FE model meshed with solid elements is appropriate, since high accuracy of finite element simulations within the theory of elasticity has been verified multiple times (see, for instance, [2]).

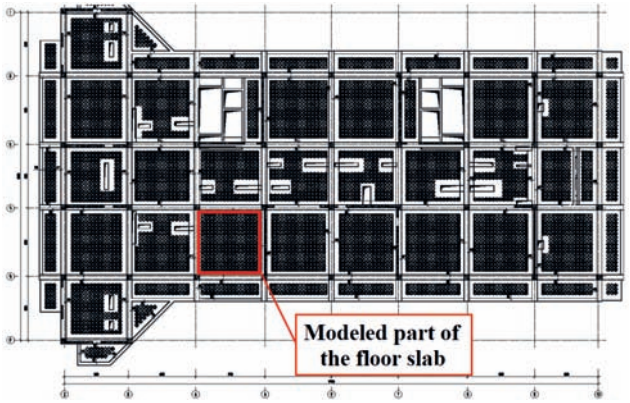


Figure 2. The drawing of a bubble deck floor slab in the reinforced concrete frame building (a part of the slab chosen for a comparative analysis of various numerical modelling techniques is outlined in red)

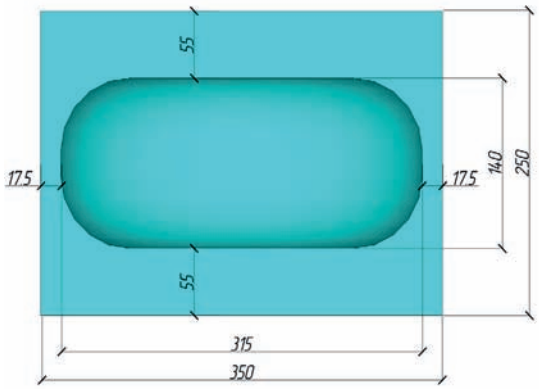


Figure 3. The cross-section of a void former cell used in the considered bubble deck floor slab

Table 1. Bubble deck floor slab material properties

Material	Elastic Modulus E, GPa	Poisson's ratio ν	Density ρ, kg/m^3
Concrete B25	30	0.2	2500

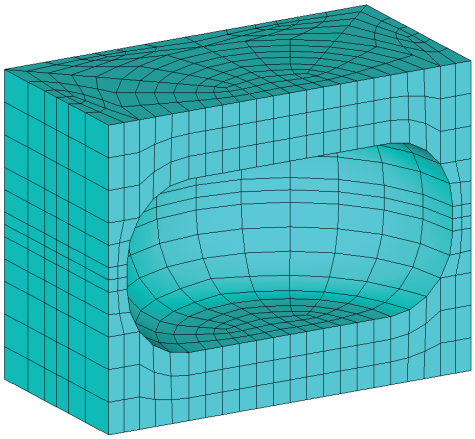


Figure 4. Mesh within the void former cell used in the reference model of the considered cast-in-place reinforced concrete bubble deck floor slab

According to the results of the first part of the present research [1], within which the modal analysis and static analysis have been performed for the models of the considered bubble deck floor slab meshed with either solid finite elements (the reference model) or structural finite elements, the closest agreement to the results calculated with the reference finite element model has been obtained for the following two cases. In the first case, the slab has been simulated as two horizontal layers of shell finite elements of the type SHELL181, in which the Reissner-Mindlin plate theory is implemented, with effective density (increased by a factor of k_ρ = 1.1484 to match the mass of the model to that of the reference model) connected together with a honey-comb structure also meshed with shell finite elements of the type SHELL181 with effective density (increased by the same factor of k_ρ = 1.1484) and effective elastic modulus (iteratively changed to match the results of the modal analysis with the reference ones) (see Table 2). In the second case, the slab has been modeled with one layer of shell finite elements of the type SHELL181 with effective density (decreased by a factor of k_ρ = 1.4376) and effective elastic modulus (see Table 3).

In the present paper, various approaches to numerical simulation of structural assembly comprised reinforced concrete bubble deck floor slab and reinforced concrete vertical load-bearing structural elements, in particular a column and wall with an embedded column, are considered.

Table 2. Parameters of the double-layer engineering finite element model

#	Element	E, GPa	ν	ρ, kg/m^3	t, mm
1	Horizontal plate of the floor slab	30	0.2	2871.1	55
2	Vertical rib of the floor slab	87	0.2	2871.1	35

Note: parameters different from the reference ones are colored in blue

Table 3. Parameters of the single-layer engineering finite element model

#	Element	E, GPa	ν	ρ, kg/m^3	t, mm
1	Floor slab	24	0.2	1739.1	250

Note: parameters different from the reference ones are colored in blue

2. PROBLEM ONE. INTERACTION OF THE BUBBLE DECK PART AND THE SOLID PART OF THE FLOOR SLAB

The reinforced concrete bubble deck floor slab, as illustrated in Fig. 5, has two distinct areas. The central part of the slab contains void formers, while the perimeter of the slab is solid to provide mechanical safety of the structural element.

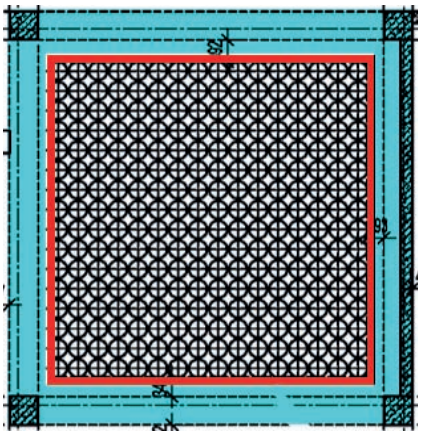


Figure 5. The simulated part of the bubble deck floor slab (the part of the slab with void formers is outlined in red, the solid area of the slab is colored in blue)

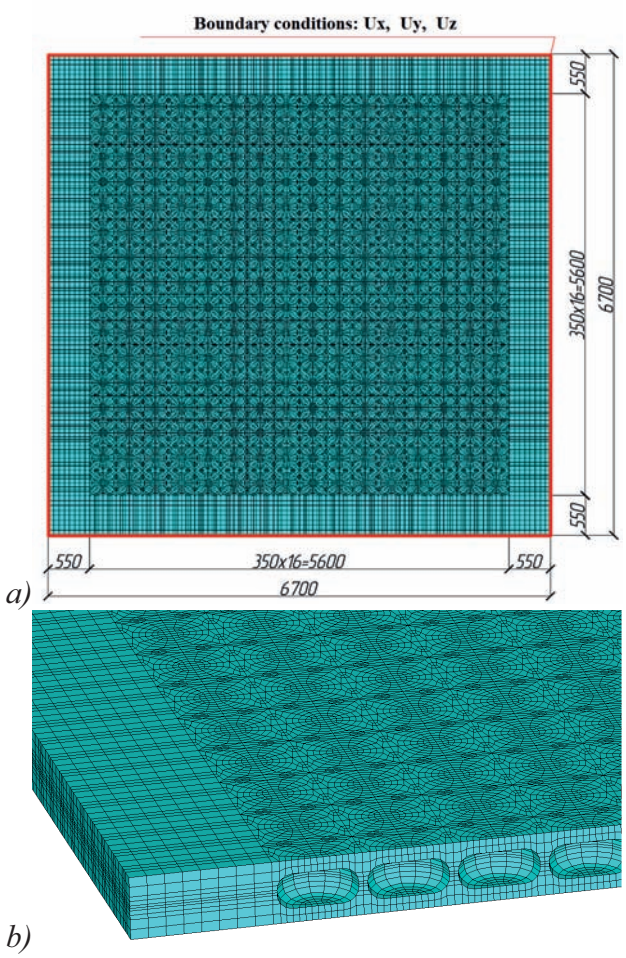


Figure 6. The numerical model meshed with solid finite elements: a) geometrical parameters and boundary conditions, b) cross-section view

To simulate various structural assemblies including bubble deck floor slab, it is necessary to accurately model transition between the part of the slab with void formers and the solid one.

A finite element model of the whole floor slab utilized for reference simulations is shown in Fig. 6. All DOFs (Ux, Uy, Uz) of the nodes located at the slab boundaries are restrained.

Two different techniques to simulate the bubble deck floor slab, including its solid part, using structural finite elements are considered.

Within the first technique, the void former cell of the slab is modelled as a honeycomb structure with top and bottom cover plates, which are all discretized through shell finite elements, while the solid part of the slab is discretized via a single layer of shell finite elements located at the middle surface (see Fig. 7).

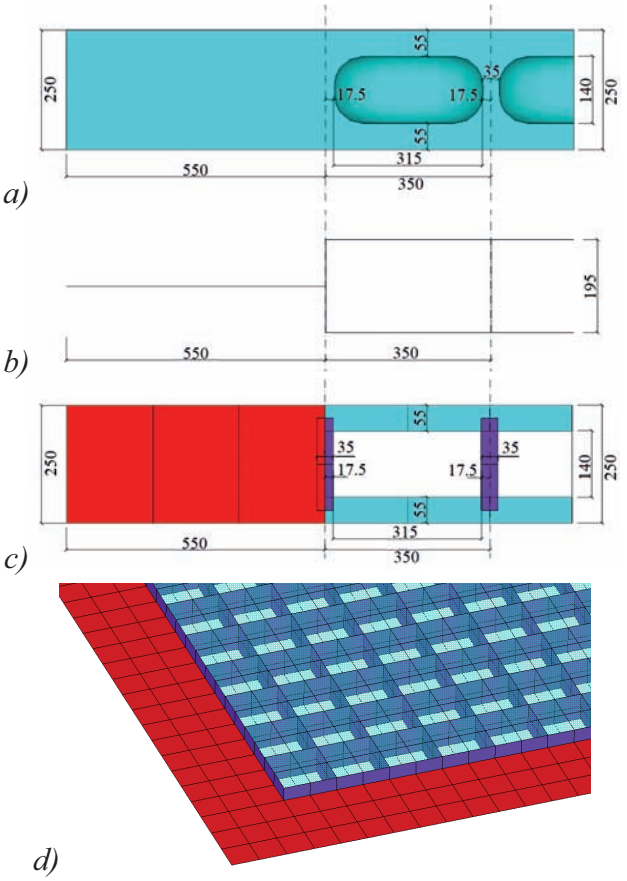


Figure 7. Finite element model for the first simulation technique: a) cross-section of the actual structure; b) computational model of the structure; c) computational model of the structure with displayed element thickness; d) orthogonal view (red – solid floor slab; light blue – cover plates of the bubble deck part of the floor slab; purple – vertical ribs of the bubble deck part of the floor slab)

With the first engineering technique (Model 1), two different sets of material properties have been adopted (see Tables 4, 5).

In the first parameter set, 1A, vertical ribs between the solid and the bubble deck parts of the floor slab have effective properties (density, elastic modulus) similar to those of other vertical ribs for parameter set 1A.

Table 4. The parameters set 1A

#	Element	E, GPa	ν	ρ, kg/m^3	t, mm
1	Horizontal plate of the bubble deck part of the floor slab	30	0.2	2871.1	55
2	Vertical rib of the bubble deck part of the floor slab	87	0.2	2871.1	35
3	Solid part of the floor slab	30	0.2	2500	250

Note: parameters different from the reference ones are colored in blue

The parameter set 1B is based onto the parameter set 1A. In the parameter set 1B, the elastic modulus of the vertical ribs between the solid part and the bubble deck parts of the floor slab elastic modulus has been significantly increased for the simulation results to match eigenfrequencies, eigenmodes, and static response of the reference model.

Table 5. The parameters set 1B

#	Element	E, GPa	ν	ρ, kg/m^3	t, mm
1	Horizontal plate of the bubble deck part of the floor slab	30	0.2	2871.1	55
2	Vertical rib of the bubble deck part of the floor slab	87	0.2	2871.1	35
3	Solid part of the floor slab	30	0.2	2500	250
4	Vertical rib at the perimeter of the bubble deck part of the floor slab	400	0.2	2871.1	35

Note: parameters different from the parameters set 1A are colored in yellow

Within the second engineering technique (Model 2), both the solid part and the bubble deck part of the floor slab are discretized through one layer of shell finite elements. To match mass, stiffness, and dynamic response characteristics of the actual structure, effective values of material properties – a parameters set 2A – have been used (see Table 6).

Table 6. The parameters set 2A

#	Element	E, GPa	ν	ρ, kg/m^3	t, mm
1	Bubble deck part of the floor slab	24	0.2	1739.1	250
2	Solid part of the floor slab	30	0.2	2500	250

Note: parameters different from the reference ones are colored in blue

In the finite element models utilized within both considered techniques, all DOFs (Ux, Uy, Uz, Rotx, Roty, Rotz) of the nodes located at the slab boundaries are restrained.
Results of the modal analyses performed using different numerical models are given in Table 7. Results of the static response analyses performed using different numerical models are presented in Tables 8, 9, and Fig. 8.

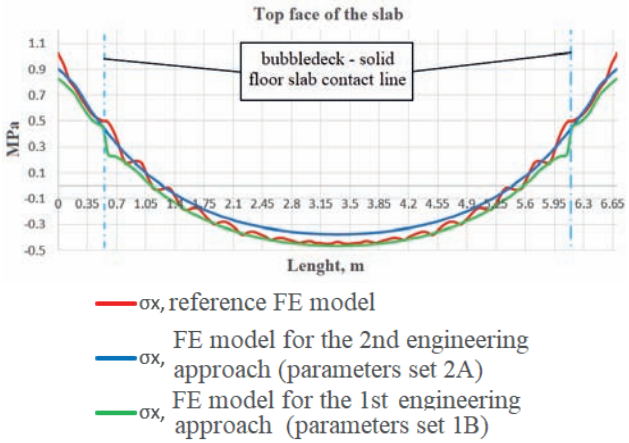


Figure 8. Normal stress along X-axis at the top face of the slab in the central cross-section due to the slab dead weight

The finite element model created within the first engineering technique using the values of the parameters given in the set 1B and the finite element model created within the second engineering approach using the values of the parameters given in the set 2A have yielded the closest agreement with the results of the modal analysis and the static response analysis obtained using the reference finite element model. The finite element model implementing the first engineering approach with the parameters set 1B has been chosen for further research.

Table 7. Results of the modal analyses (In brackets given are the discrepancy, in percent, from the results obtained with the reference finite element model)

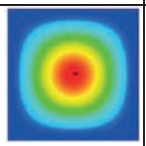
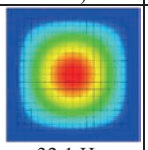
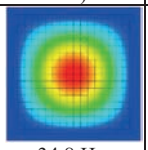
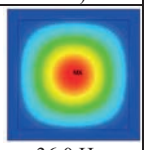
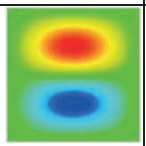
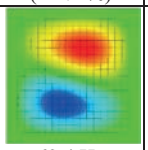
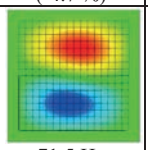
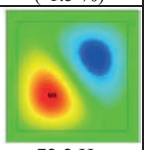
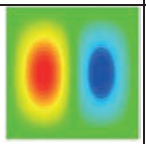
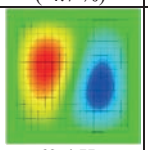
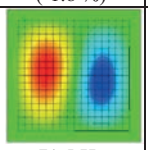
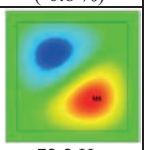
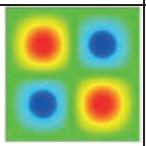
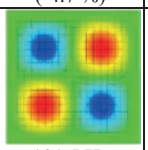
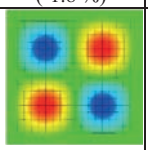
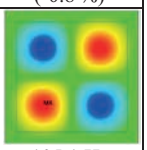
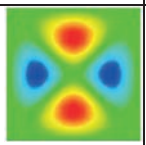
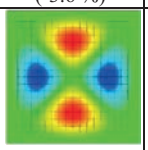
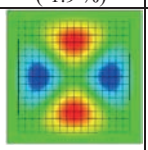
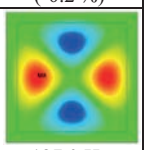
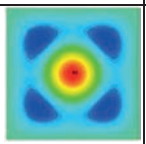
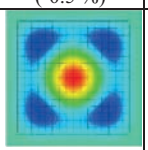
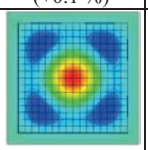
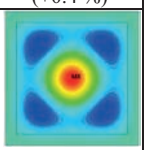
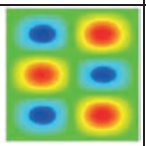
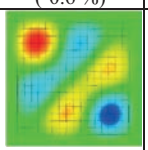
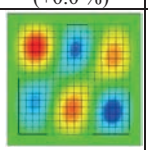
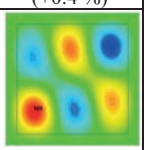
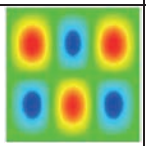
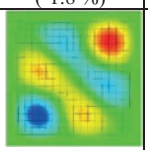
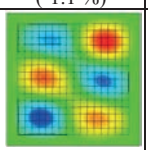
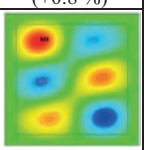
#	Reference model	Model 1 (parameters set 1A)	Model 1 (parameters set 1B)	Model 2 (parameters set 2A)
1	 36.6 Hz	 32.1 Hz (-12.1 %)	 34.8 Hz (-4.7 %)	 36.0 Hz (-1.5 %)
2	 72.8 Hz	 69.4 Hz (-4.7 %)	 71.5 Hz (-1.8 %)	 72.2 Hz (-0.8 %)
3	 72.8 Hz	 69.4 Hz (-4.7 %)	 71.5 Hz (-1.8 %)	 72.2 Hz (-0.8 %)
4	 105.3 Hz	 101.5 Hz (-3.6 %)	 103.3 Hz (-1.9 %)	 105.1 Hz (-0.2 %)
5	 126.5 Hz	 125.9 Hz (-0.5 %)	 126.7 Hz (+0.1 %)	 127.0 Hz (+0.4 %)
6	 127.2 Hz	 126.4 Hz (-0.6 %)	 127.2 Hz (+0.0 %)	 127.7 Hz (+0.4 %)
7	 156.2 Hz	 153.4 Hz (-1.8 %)	 154.5 Hz (-1.1 %)	 157.4 Hz (+0.8 %)
8	 156.2 Hz	 153.4 Hz (-1.8 %)	 154.5 Hz (-1.1 %)	 157.4 Hz (+0.8 %)

Table 8. Comparison of the vertical displacements due to the slab dead weight (In brackets given are the discrepancy, in percent, from the results obtained with the reference finite element model)

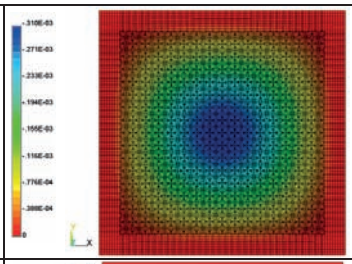
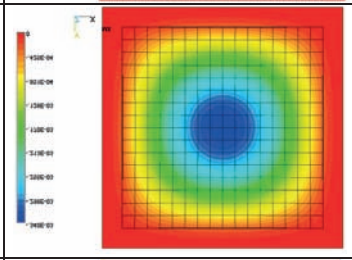
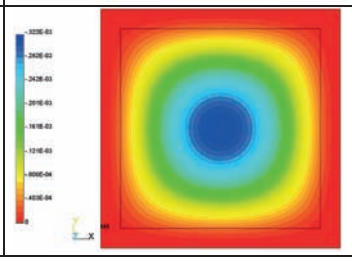
Reference model		Uz_{max} = -0.31 mm
Model 1 (parameters set 1B)		Uz_{max} = -0.34 mm (-9.7%)
Model 2 (parameters set 2A)		Uz_{max} = -0.32 mm (-3.2%)

Table 9. Comparison of the normal stress along X-axis at the top face of the slab in the central cross-section due to the slab dead weight (see also Fig. 8)

Finite element model	Min σ_x, Pa	Δ, %	Max σ_x, Pa	Δ, %
Reference model	-448349	-	1025472	-
Model 1 (parameters set 1B)	-466473	-4	831076	-19
Model 2 (parameters set 2A)	-376800	+16	901916.2	-12

3. PROBLEM TWO. A STRUCTURAL ASSEMBLY COMPRISING A BUBBLE DECK FLOOR SLAB AND A COLUMN

The second formulated problem deals with simulation of a structural assembly comprising a

bubble deck floor slab and a column using shell and beam finite elements for its spatial discretization. To determine the most accurate and efficient engineering technique for this problem, several models based on shell finite elements have been assembled and tested. Accuracy and efficiency of the particular engineering technique has been evaluated through comparison of the results of modal analysis with those obtained using a reference finite element model. As in the first case considered in the present work, as well as in the first part of the research [1], the reference model is the one constructed using solid finite elements. The reference finite element model is shown in Fig. 9.

According to the solution of the first problem describe in the previous section, the constructed engineering models are all based onto representation of the bubble deck part of the floor slab as a honey-comb structure covered with top and bottom plates, and discretization of the solid part of the floor slab with one layer of shell finite elements located at its middle surface. A total of three engineering models have been constructed, which use the same mesh (shown in Fig. 10) and differ from each other only in their parameter values.

The first parameters set, 1A, (see Table 10) is based onto the parameters set 1A from the previous section (see Table 4) with an extension to include column parameters.

In the second parameters set, 1B, (see Table 11) which is based onto the parameters set 1A, an area of the floor slab within the projection of the column cross-section (see Fig. 11) has the Young's modulus several orders of magnitude greater than that for the rest of the slab to more precisely simulate a column-slab intersection which response within the considered problem is close the rigid body one.

In the third parameters set, 1C, (see Table 12) the Young's modulus of the vertical ribs at the perimeter of the bubble deck part of the floor slab (see Fig. 11) has been increased by several times, like in the parameters set 1B of the previous section (see Table 5).

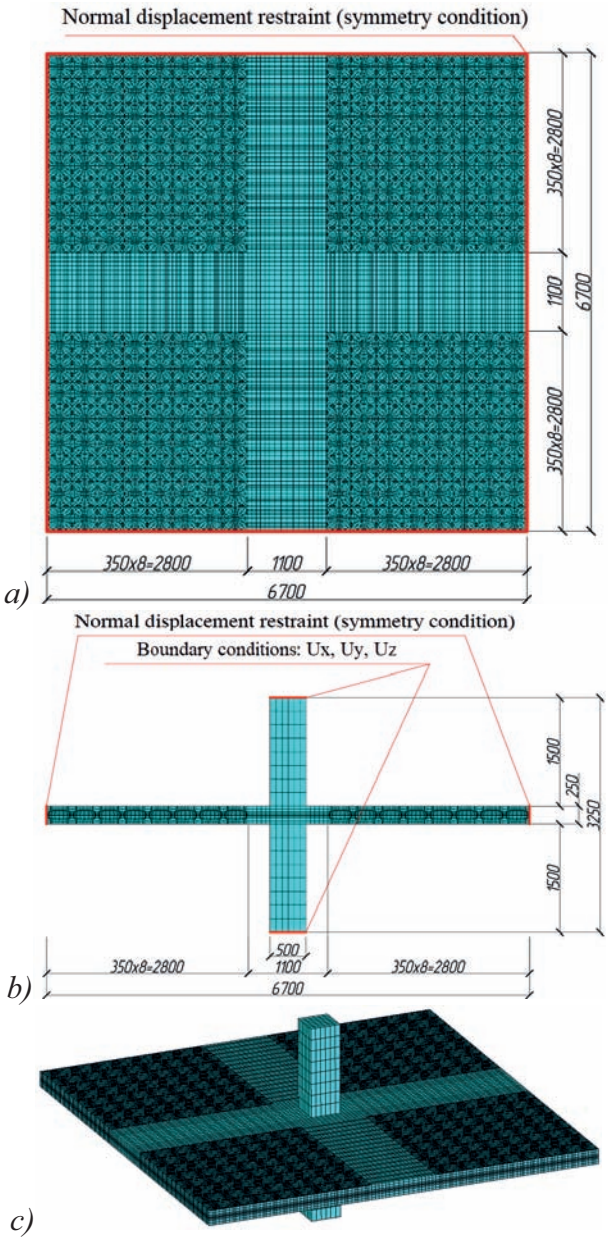


Figure 9. Geometrical parameters and boundary conditions (red lined) of the reference model of the structural assembly comprising the bubble deck floor slab and the column: a) top view; b) side view; c) orthogonal view

All DOFs (Ux, Uy, Uz, Rotx, Roty, Rotz for the models constructed using shell and beam finite elements and Ux, Uy, Uz for the reference model discretized with solid finite elements) of the nodes located at the column top and bottom are restrained. Boundary conditions at the simulated slab perimeter take into account symmetry of the problem, in particu-

lar horizontal displacements in the normal direction to a corresponding edge are restrained.

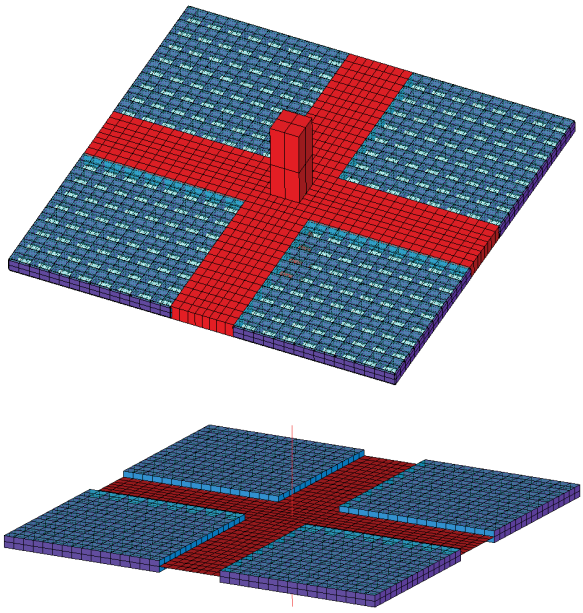


Figure 10. Finite element mesh used to simulate the structural assembly comprising the bubble deck floor slab and the column: a) element thickness displayed; b) element thickness is not displayed

Table 10. The parameters set 1A

#	Element	E, GPa	ν	ρ, kg/m^3	t, mm
1	Horizontal plate of the bubble deck part of the floor slab	30	0.2	2871.1	55
2	Vertical rib of the bubble deck part of the floor slab	87	0.2	2871.1	35
3	Solid part of the floor slab	30	0.2	2500	250
4	Column	30	0.2	2500	500×500

Note: parameters different from the reference ones are colored in blue

The results of the modal analysis of the structural assembly comprising the bubble deck floor slab and the column are given in Table 13. The engineering finite element model used in conjunction with the parameters set 1C (see in Table 11) has yielded the closest agreement with the eigenproblem solution obtained using the reference finite element model discretized with solid finite elements. The largest discrepancy amounts to 5%.

Table 11. The parameters set 1B

#	Element	E, GPa	ν	ρ, kg/m^3	t, mm
1	Horizontal plate of the bubble deck part of the floor slab	30	0.2	2871.1	55
2	Vertical rib of the bubble deck part of the floor slab	87	0.2	2871.1	35
3	Solid part of the floor slab	30	0.2	2500	250
4	Column	30	0.2	2500	500×500
5	Floor slab within the projection of the column cross-section	3e06	0.2	0	250

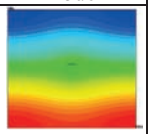
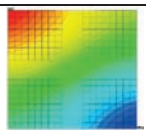
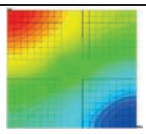
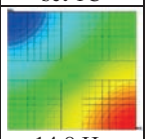
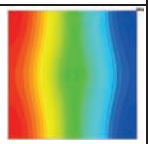
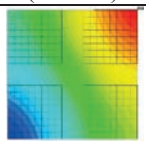
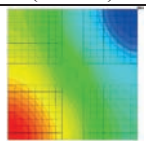
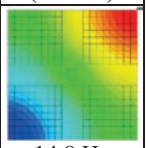
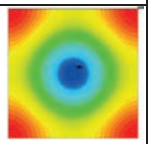
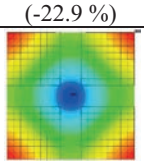
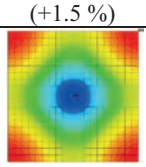
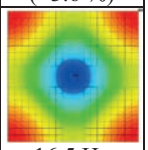
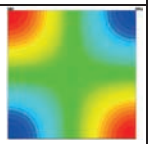
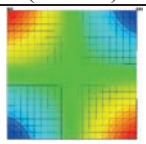
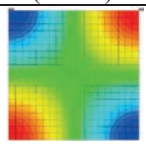
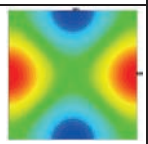
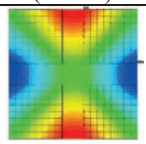
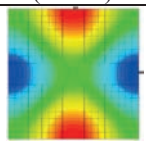
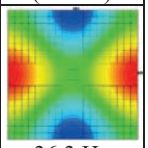
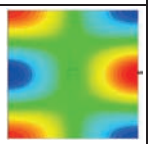
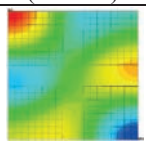
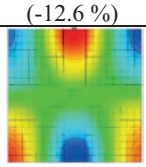
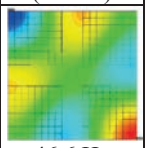
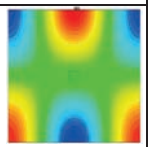
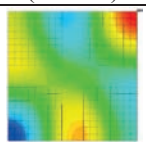
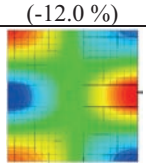
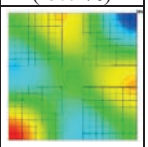
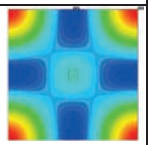
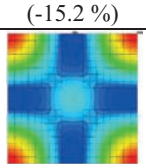
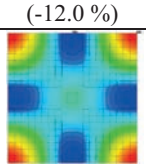
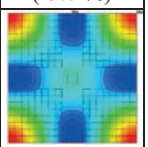
Note: parameters different from the parameters set 1A are colored in yellow

Table 12. The parameters set 1C

#	Element	E, GPa	ν	ρ, kg/m^3	t, mm
1	Horizontal plate of the floor slab	30	0.2	2871.1	55
2	Vertical rib of the floor slab	87	0.2	2871.1	35
3	Solid part of the floor slab	30	0.2	2500	250
4	Column	30	0.2	2500	500×500
5	Floor slab within the projection of the column cross-section	3e06	0.2	0	250
6	Vertical rib at the perimeter of the bubble deck part of the floor slab	400	0.2	2871.1	35

Note: parameters different from the parameters set 1B are colored in yellow

Table 13. Results of the modal analysis (In brackets given are the discrepancy, in percent, from the results obtained with the reference finite element model)

#	Reference model	Parameter set 1A	Parameter set 1B	Parameter set 1C
1	 14.3 Hz	 11.0 Hz (-22.9 %)	 14.5 Hz (+1.5 %)	 14.8 Hz (+3.6 %)
2	 14.3 Hz	 11.0 Hz (-22.9 %)	 14.5 Hz (+1.5 %)	 14.8 Hz (+3.6 %)
3	 16.3 Hz	 13.9 Hz (-15.1 %)	 15.4 Hz (-5.4 %)	 16.5 Hz (+1.3 %)
4	 20.5 Hz	 19.6 Hz (-4.1 %)	 20.1 Hz (-1.7 %)	 20.3 Hz (-0.7 %)
5	 37.4 Hz	 31.9 Hz (-14.7 %)	 32.7 Hz (-12.6 %)	 36.3 Hz (-3.1 %)
6	 49.1 Hz	 41.6 Hz (-15.2 %)	 43.2 Hz (-12.0 %)	 46.6 Hz (-5.0 %)
7	 49.1 Hz	 41.6 Hz (-15.2 %)	 43.2 Hz (-12.0 %)	 46.6 Hz (-5.0 %)
8	 58.6 Hz	 50.0 Hz (-14.7 %)	 52.7 Hz (-10.1 %)	 56.11 Hz (-4.3 %)
…	…	…	…	…

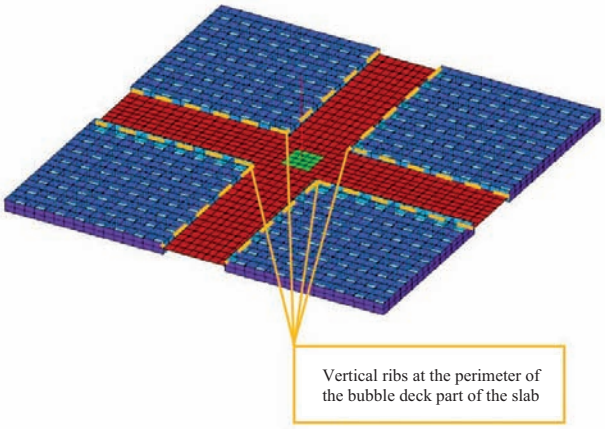


Figure 11. The finite element model used in conjunction with the parameters set 1C (finite elements within the projection of the column cross-section are colored in green)

4. PROBLEM THREE. A STRUCTURAL ASSEMBLY COMPRISING A BUBBLE DECK FLOOR SLAB AND A WALL WITH AN EMBEDDED COLUMN

Another problem considered in the present paper deals with simulation of a structural assembly comprising a bubble deck floor slab and a wall with an embedded column using shell and beam finite elements for its spatial discretization. Three engineering approaches have been tested to determine the most accurate and efficient one. Accuracy and efficiency of the particular engineering technique has been evaluated through comparison of the results of modal analysis with those obtained using a reference finite element model. As in the first two cases considered in the present work, as well as in the first part of the research [1], the reference model is the one constructed using solid finite elements. Geometrical parameters and spatial discretization of the reference finite element model are given in Fig. 12.

All DOFs (Ux, Uy, Uz, Rotx, Roty, Rotz for the models constructed using shell and beam finite elements and Ux, Uy, Uz for the reference model discretized with solid finite elements) of the nodes located at the column top and bottom are restrained. Boundary conditions at the simulated slab perimeter take into account symmetry of

the problem, in particular horizontal displacements in the normal direction to a corresponding edge are restrained.

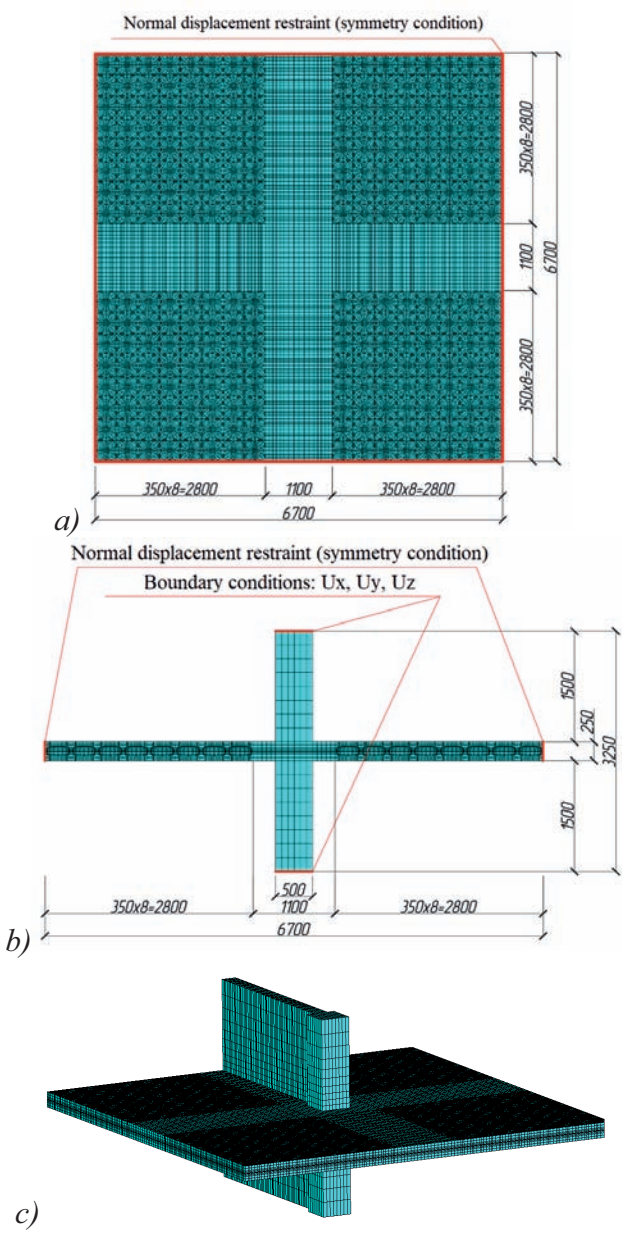


Figure 12. Geometrical parameters and boundary conditions (red lined) of the reference model of the structural assembly comprising the bubble deck floor slab and the wall with the embedded column: a) top view; b) side view; c) orthogonal view

The engineering finite element model used to solve the considered problem is based onto the model constructed in the previous section with the only difference that the wall has been added (see Fig. 13). As in the previous case, a difference between the three tested engineering techniques concerns values of the parameters defined in each case (see Tables 14–16).

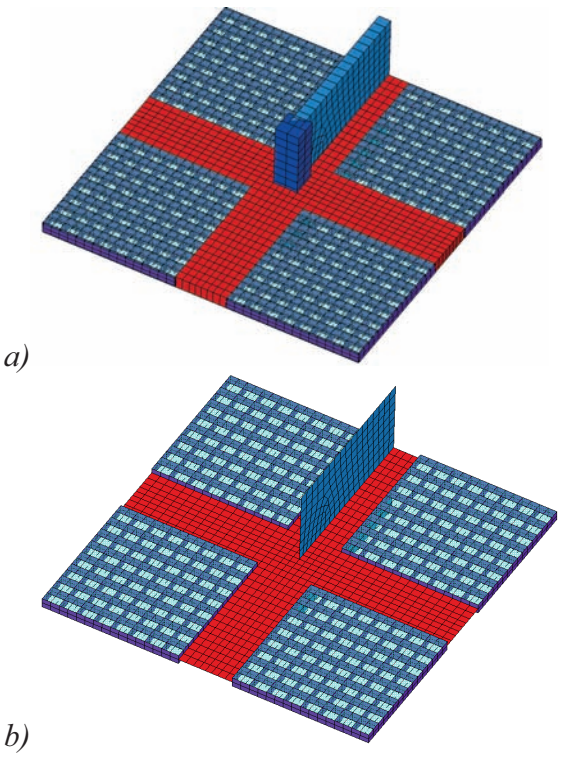


Figure 13. Finite element mesh used to simulate the structural assembly comprising the bubble deck floor slab and the wall with the embedded column: a) element thickness displayed; b) element thickness is not displayed

Table 14. The parameters set 1A

#	Element	*E*, GPa	*v*	*ρ*, kg/m^3	*t*, mm
1	Horizontal plate of the bubble deck part of the floor slab	30	0.2	2871.1	55
2	Vertical rib of the bubble deck part of the floor slab	87	0.2	2871.1	35
3	Solid part of the floor slab	30	0.2	2500	250
4	Column	30	0.2	2500	500×500
5	Wall	30	0.2	2500	250

Note: parameters different from the reference ones are colored in blue

Table 15. The parameters set 1B

#	Element	E, GPa	ν	ρ, kg/m^3	t, mm
1	Horizontal plate of the bubble deck part of the floor slab	30	0.2	2871.1	55
2	Vertical rib of the bubble deck part of the floor slab	87	0.2	2871.1	35
3	Solid part of the floor slab	30	0.2	2500	250
4	Column	30	0.2	2500	500×500
5	Wall	30	0.2	2500	250
6	Floor slab within the projection of the column cross-section	3e06	0.2	0	250

Note: parameters different from the parameters set 1A are colored in yellow

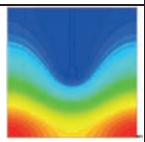
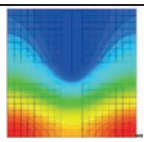
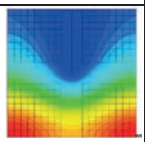
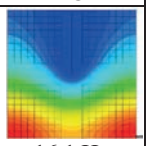
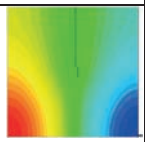
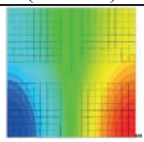
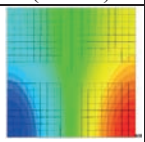
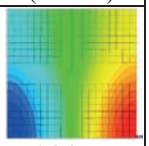
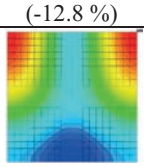
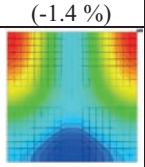
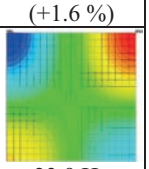
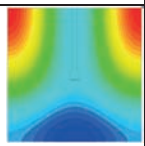
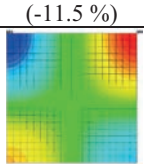
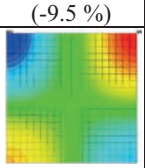
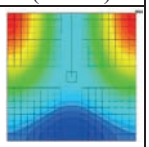
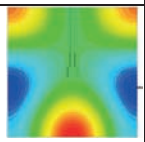
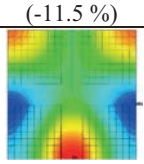
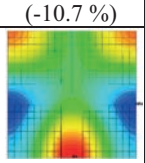
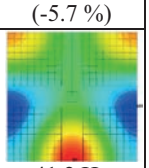
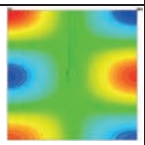
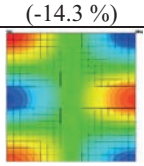
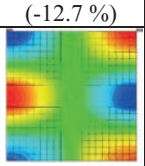
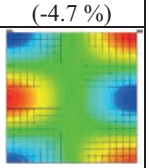
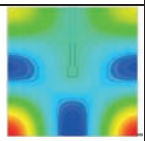
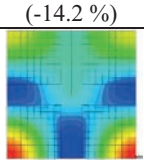
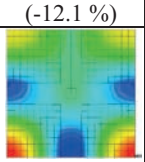
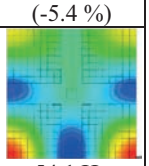
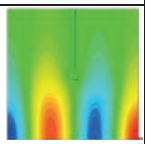
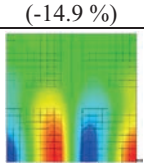
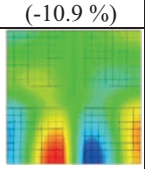
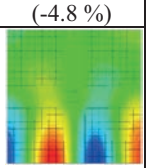
Table 16. The parameters set 1C

#	Element	E, GPa	ν	ρ, kg/m^3	t, mm
1	Horizontal plate of the bubble deck part of the floor slab	30	0.2	2871.1	55
2	Vertical rib of the bubble deck part of the floor slab	87	0.2	2871.1	35
3	Solid part of the floor slab	30	0.2	2500	250
4	Column	30	0.2	2500	500×500
5	Wall	30	0.2	2500	250
6	Floor slab within the projection of the column cross-section	3e06	0.2	0	250
7	Vertical rib at the perimeter of the bubble deck part of the floor slab	400	0.2	2871.1	35

Note: parameters different from the parameters set 1B are colored in yellow

The results of the modal analysis of the structural assembly comprising the bubble deck floor slab and the wall with the embedded column are given in Table 17. The engineering model used in conjunction with the parameters set 1C (see in Table 16) has yielded the closest agreement with the solution obtained using the reference finite element model discretized with solid finite elements. The largest discrepancy amounts to 5.7%.

Table 17. Results of the modal analysis (In brackets given are the discrepancy, in percent, from the results obtained with the reference finite element model)

#	Reference model	Parameter set 1A	Parameter set 1B	Parameter set 1C
1	 15.8 Hz	 13.1 Hz (-17.0 %)	 15.3 Hz (-2.9 %)	 16.1 Hz (+2.2 %)
2	 16.1 Hz	 14.1 Hz (-12.8 %)	 15.9 Hz (-1.4 %)	 16.4 Hz (+1.6 %)
3	 24.9 Hz	 22.0 Hz (-11.5 %)	 22.6 Hz (-9.5 %)	 23.9 Hz (-4.0 %)
4	 25.9 Hz	 22.9 Hz (-11.5 %)	 23.1 Hz (-10.7 %)	 24.4 Hz (-5.7 %)
5	 43.2 Hz	 37.1 Hz (-14.3 %)	 37.7 Hz (-12.7 %)	 41.2 Hz (-4.7 %)
6	 50.3 Hz	 43.1 Hz (-14.2 %)	 44.2 Hz (-12.1 %)	 47.6 Hz (-5.4 %)
7	 56.8 Hz	 48.4 Hz (-14.9 %)	 50.6 Hz (-10.9 %)	 54.1 Hz (-4.8 %)
8	 93.5 Hz	 81.7 Hz (-12.6 %)	 84.3 Hz (-9.8 %)	 91.8 Hz (-1.8 %)

CONCLUSION

The following conclusions can be made based on the first part of the research [1], the present paper, and their comparison:

1. Three types of finite element models have been constructed to perform static response analysis and modal analysis of a reinforced concrete bubble deck floor slab as a separate unit or as a part of a structural assembly comprising the slab and a column or the slab and a wall with an embedded column:

– Models of the first type have been spatially discretized with solid finite elements, that has allowed one to precisely repeat the bubble deck floor slab geometry. Numerical results obtained with such models have been considered as reference ones.

– Models of the second type have been spatially discretized with shell and beam finite elements. In these models the void former cell of the slab is modelled as a honey-comb structure with top and bottom cover plates.

– Models of the third type have also been spatially discretized with shell and beam finite elements, but in these models the part of the floor slab with void formers is modelled through one layer of shell finite elements located at the slab middle surface and been assigned effective mass and stiffness properties.

2. Numerical models based on solid finite elements allow one to accurately simulate static and dynamic responses of structural elements with a complex cross-section, like the considered bubble deck floor slab. Yet, application of such an approach to a building arises enormous difficulties during model construction and is very time consuming at the analysis stage. Moreover, common tools to design reinforcement are not applicable within such an approach.
3. The engineering approach, within which the void former cell of the slab is modelled as a honeycomb structure with top and bottom cover plates, all discretized with shell finite elements, significantly reduces human and computational resources necessary to construct and analyze the model of a building, in which the considered lightweight structural solution is adopted. It provides sufficient accuracy and allows one to use standard design tools, in particular to determine the required amount of reinforcement. This developed technique is recommended to be utilized for simulation of building with similar lightweight structural elements solutions, in particular located in earthquake-prone regions.
4. The engineering approach, in which the reinforced concrete bubble deck floor slab is modelled with one layer of shell finite elements located at the slab middle surface and been assigned effective mass and stiffness properties, provides relatively low accuracy with respect to both static and dynamic responses of such structural elements and assemblies comprising them, and, given the more accurate alternative exists, should not be utilized for simulation of buildings with bubble deck floor slabs exposed to seismic loads.

ACKNOWLEDGEMENTS

The research was conducted as part of the development programme for 2025-2036 of Moscow State University of Civil Engineering under the framework of strategic academic leadership programme “Priority 2030”.

REFERENCES

1. **Belostotsky A., Nagibovich A., Scherbina S., Vasileva T.** Numerical modeling of cast-in-place reinforced concrete bubble deck floor slabs utilized in earthquake-prone region // Int. J. Comput. Civil Struct. Eng. – 2025. – Vol. 21. – No. 2. – Pp. 187-199.
2. **Dzhamuev B.K.** The effect of non-removable void generators on the strength of monolithic reinforced concrete floor slabs clamped along the contour // Building and Reconstruction. – 2024. – Vol. 2. Pp. 3-15. (In Russian)

3. **Tiwari N., Zafar S.** Structural behavior of bubble deck slabs and its application: Main paper // Int. J. Sci. Res. Dev. – 2016. – Vol. 4. – Iss. 02. – Pp. 433-437.
4. **Ibrahim A.M., Ali N.K., Salman W.D.** Flexural capacities of reinforced concrete two-way bubble deck slabs of plastic spherical voids // J. Print. Iraq. – 2013. – Vol. 06. – No. 02. – Pp: 9-20.
5. **Valivonis J., Skuturna T, Daugeviius M., Šneideris A.** Punching shear strength of reinforced concrete slabs with plastic void formers // Constr. Build. Mater. – 2017. – Vol.145. – Pp. 518-527.
6. **Saifulla M., Azeem M.A.** Comparative seismic performance of a conventional slab and flat slab over a bubble deck slab // Int. J. Emerg. Technol. Adv. Eng. – 2017. – Vol. 7. – Iss. 11. – Pp. 137-143.
7. **Teja P.P., Kumar P.V, Mounika C.H., Saha P.** Structural behavior of bubble deck slab / In: Proceedings of the IEEE-International Conference on Advances in Engineering, Science and Management, Nagapattinam, Tamil Nadu, India, 2012. – Pp: 383-388.
8. **Lakshmikanth L., Poluraju P.** Performance of structural behaviour of bubble deck slab // Int. J. Recent Technol. Eng. – 2019. – Vol.7. – Iss. 6C2. – Pp. 865-870.
9. **Varghese J.P, George M.** Parametric investigation on the seismic response of voided and solid flat slab systems // Int. J. Innov. Sci. Eng. Technol. – 2018. – Vol. 5. – Iss. 3. – Pp 256-258.
10. **Nagashree B, Shariff S., Kumar M.** Experimental studies on comparison of conventional slab and bubble deck slab based on strength // Int. J. Sci. Res. Dev. – 2017. – Vol. 5. – Iss. 3. – Pp: 1160-1162.
11. **Orlova M.D., Mnushkin M.A., Evtushenko I.S., Vinogradova K.I., Egarmin K.A.** Analysis of the use of hollow formers from recycled polypropylene in the creation of lightweight monolithic floors. Research of various directions of modern science: Collection of materials of the XXI International Scientific and practical Conference. Part 1. Moscow. 2017. Pp. 562-567. (In Russian)
12. **Filimonova E.S**. Analysis of the stress-strain state of a monolithic floor slab with void generators according to the Cobiax system based on various computational models // Young Scientist. – 2022. – No. 20 (415). – Pp. 107-109. (In Russian)
13. STO 35546020.001-2016 «Fixed formwork (voids and couplings) Sibforma ®. General information about the technology, product range. Recommendations for the calculation and design of monolithic girderless floor slabs with non-removable formwork Sibform ® in accordance with Code of Practice 63.13330.2012». (In Russian)
14. STO 38311046-001-2019 «Monolithic reinforced concrete lightweight slabs with Simkar void formers. Rules of design and construction». (In Russian)
15. Recommendations for the calculation of monolithic beamless floor slabs with Simkar void-forming slabs (without prestressing) / National Research Moscow State University of Civil Engineering, 2014. – 119 p.
16. **Белостоцкий А.М., Дубинский С.И., Аул А.А., Нагибович А.И., Афанасьева И.Н., Козырев О.А., Павлов А.С.** Verification report ANSYS Mechanical software (4 volume). – M.: National Research Moscow State University of Civil Engineering, Research & Development Centre StaDyO, 2009, 2024.
17. Code of Practice 63.13330.2018 “Concrete and reinforced concrete structures. General provisions”.
18. Structural Analysis Guide, Documentation for ANSYS, Release 21R2. 2021.
19. **Belostotsky A., Nagibovich A., Novikov P., Vershinin V.** Earthquake of buildings and structures: regulatory “must-do” or scientifically substantiated results // Int. J. Comput. Civil Struct. Eng. – 2024. – Vol. 20. – No. 4. – Pp. 241-252.

20. **Dmitriev D., Novikov P., Petryashev S., Nagibovich A.** Consideration of the seismic impact's wave nature in the design justification of high-rise buildings seismic resistance // Int. J. Comput. Civil Struct. Eng. – 2024. – Vol. 20. – No. 3. – Pp. 198-205.
21. **Belostotsky A., Nagibovich A., Pavlov A.** Numerical simulation of the stress-strain state of a large-span structure with joints with gap under the seismic loads in a transient dynamic // Int. J. Comput. Civil Struct. Eng. – 2023. – Vol. 19. – No. 3. – Pp. 165-172.
22. **Malahova A.N**. Pustotnye kessonnye plity perekrytij monolitnyh mnogoetazhnyh zdanij [Hollow coffered floor slabs of monolithic multi-storey buildings] // Vestnik MGSU. – 2016. – No. 6. – Pp. 15-24. (In Russian)

СПИСОК ЛИТЕРАТУРЫ

1. **Belostotsky A., Nagibovich A., Scherbina S., Vasileva T.** Numerical modeling of cast-in-place reinforced concrete bubble deck floor slabs utilized in earthquake-prone region // Int. J. Comput. Civil Struct. Eng. – 2025. – Vol. 21. – No. 2. – P. 187-199.
2. **Джамуев Б.К.** Влияния несъемных пустотообразователей на прочность защемленных по контуру монолитных железобетонных плит перекрытия // Строительство и реконструкция. –2024. – Т. 2. – С. 3-15.
3. **Tiwari N., Zafar S.** Structural behavior of bubble deck slabs and its application: Main paper // Int. J. Sci. Res. Dev. – 2016. – Vol. 4. – Iss. 02. – Pp. 433-437.
4. **Ibrahim A.M., Ali N.K., Salman W.D.** Flexural capacities of reinforced concrete two-way bubble deck slabs of plastic spherical voids // J. Print. Iraq. – 2013. – Vol. 06. – No. 02. – Pp: 9-20.
5. **Valivonis J., Skuturna T, Daugeviius M., Šneideris A.** Punching shear strength of reinforced concrete slabs with plastic void formers // Constr. Build. Mater. – 2017. – Vol.145. – Pp. 518-527.
6. **Saifulla M., Azeem M.A.** Comparative seismic performance of a conventional slab and flat slab over a bubble deck slab // Int. J. Emerg. Technol. Adv. Eng. – 2017. – Vol. 7. – Iss. 11. – Pp. 137-143.
7. **Teja P.P., Kumar P.V, Mounika C.H., Saha P.** Structural behavior of bubble deck slab / In: Proceedings of the IEEE-International Conference on Advances in Engineering, Science and Management, Nagapattinam, Tamil Nadu, India, 2012. – Pp: 383-388.
8. **Lakshmikanth L., Poluraju P.** Performance of structural behaviour of bubble deck slab // Int. J. Recent Technol. Eng. – 2019. – Vol.7. – Iss. 6C2. – Pp. 865-870.
9. **Varghese J.P, George M.** Parametric investigation on the seismic response of voided and solid flat slab systems // Int. J. Innov. Sci. Eng. Technol. – 2018. – Vol. 5. – Iss. 3. – Pp 256-258.
10. **Nagashree B, Shariff S., Kumar M.** Experimental studies on comparison of conventional slab and bubble deck slab based on strength // Int. J. Sci. Res. Dev. – 2017. – Vol. 5. – Iss. 3. – Pp: 1160-1162.
11. **Орлова М.Д., Мнушкин М.А., Евтушенко И.С., Виноградова К.И., Егармин К.А.** Анализ применения пустотообразователей из рециклированного полипропилена при создании облегченных монолитных перекрытий. Исследование различных направлений современной науки: Сборник материалов XXI Международной научнопрактической конференции. Ч.1. Москва. 2017. С. 562-567.
12. **Филимонова Е.С.** Анализ напряженно-деформированного состояния монолитной плиты перекрытия с пустотообразователями по системе Cobiax на основании различных расчетных моделей // Молодой ученый. – 2022. – № 20 (415). – С. 107-109.

13. СТО 35546020.001-2016 «Несъемная опалубка (пустотообразователи и соединительные муфты) Сибформа®. Общие сведения о технологии, номенклатура изделий. Рекомендации по расчету и конструированию монолитных безбалочных плит перекрытий с несъемной опалубкой Сибформа® в соответствии с СП 63.13330.2012».
14. СТО 38311046-001-2019 «Монолитные железобетонные облегченные плиты с пустотообразователями Simkar. Правила проектирования и возведения».
15. Рекомендации по расчету монолитных безбалочных плит перекрытий с пустотообразователями «Симкар» (без предварительного напряжения) / ФБГОУ ВПО «МГСУ». – М.: МГСУ, 2014. –119 с.
16. **Белостоцкий А.М., Дубинский С.И., Аул А.А., Нагибович А.И., Афанасьева И.Н., Козырев О.А., Павлов А.С.** Верификационный отчет по программному комплексу ANSYS Mechanical (4 тома). – М.: ЗАО НИЦ СтаДиО, НОЦ КМ МГСУ, 2009, 2024.
17. СП 63.13330.2018. Бетонные и железобетонные конструкции. М., Минстрой, 2018.
18. Structural Analysis Guide, Documentation for ANSYS, Release 21R2. 2021.
19. **Belostotsky A., Nagibovich A., Novikov P., Vershinin V.** Earthquake of buildings and structures: regulatory “must-do” or scientifically substantiated results // Int. J. Comput. Civil Struct. Eng. – 2024. – Vol. 20. – No. 4. – Pp. 241-252.
20. **Dmitriev D., Novikov P., Petryashev S., Nagibovich A.** Consideration of the seismic impact’s wave nature in the design justification of high-rise buildings seismic resistance // Int. J. Comput. Civil Struct. Eng. – 2024. – Vol. 20. – No. 3. – Pp. 198-205.
21. **Belostotsky A., Nagibovich A., Pavlov A.** Numerical simulation of the stress-strain state of a large-span structure with joints with gap under the seismic loads in a transient dynamic // Int. J. Comput. Civil Struct. Eng. – 2023. – Vol. 19. – No. 3. – Pp. 165-172.
22. **Малахова А.Н.** Пустотные кессонные плиты перекрытий монолитных многоэтажных зданий // Вестник МГСУ. – 2016. – № 6. – С. 15-24

Alexander M. Belostotsky – DSc, Professor, Full Member of the Russian Academy of Architecture and Construction Sciences, Scientific adviser at Zolotov Research and Educational Center for Computational Modelling of the National Research Moscow State University of Civil Engineering; 129337, Russia, Moscow, Yaroslavskoe shosse, 26. E-mail: amb@stadyo.ru

Белостоцкий Александр Михайлович – д.т.н., профессор, академик РААСН, научный руководитель НОЦ КМ им. А.Б. Золотова Национального исследовательского Московского государственного строительного университета; 129337, Россия, г. Москва, Ярославское шоссе, д. 26. E-mail: amb@stadyo.ru

Alexander I. Nagibovich – engineer at Zolotov Research and Educational Center for Computational Modelling of the National Research Moscow State University of Civil Engineering; 129337, Russia, Moscow, Yaroslavskoe shosse, 26. Leading calculation engineer at the Scientific and Research Center StaDyO; 18, The 3rd Yamskogo Polya st., Moscow, 125040, Russia. E-mail: nagibovich@yandew.ru

Нагибович Александр Игоревич – к.т.н., старший научный сотрудник НОЦ КМ им. А.Б. Золотова Национального исследовательского Московского государственного строительного университета; 129337, Россия, г. Москва, Ярославское шоссе, д. 26. Ведущий инженер-расчетчик АО НИЦ СтаДиО; E-mail: nagibovich@yandex.ru

Sergey V. Scherbina – engineer at Zolotov Research and Educational Center for Computational Modelling of the National Research Moscow State University of Civil Engineering; 129337, Russia, Moscow, Yaroslavskoe shosse, 26. Calculation engineer at the Scientific and Research Center StaDyO; 18, The 3rd Yamskogo Polya st., Moscow, 125040, Russia. E-mail: scherbine@mail.ru

Щербина Сергей Викторович – инженер НОЦ КМ им. А.Б. Золотова Национального исследовательского Московского государственного строительного университета; 129337, Россия, г. Москва, Ярославское шоссе, д. 26. Инженер-расчетчик АО НИЦ СтаДиО; E-mail: scherbine@mail.ru

Tatiana N. Vasileva – engineer at Zolotov Research and Educational Center for Computational Modelling of the National Research Moscow State University of Civil Engineering; 129337, Russia, Moscow, Yaroslavskoe shosse, 26. Calculation engineer at the Scientific and Research Center StaDyO; 18, The 3rd Yamskogo Polya st., Moscow, 125040, Russia. E-mail: rabitfew@gmail.com

Васильева Татьяна Николаевна – инженер НОЦ КМ им. А.Б. Золотова Национального исследовательского Московского государственного строительного университета; 129337, Россия, г. Москва, Ярославское шоссе, д. 26. Инженер-расчетчик АО НИЦ СтаДиО; E-mail: rabitfew@gmail.com